ELSEVIER

Journal of Alloys and Compounds 279 (1998) 220–228

Journal of ALLOYS AND COMPOUNDS

The effects of Ag addition and magnetic field on melt-processed $YBa_2Cu_3O_x$ superconductors

A. Ateş, E. Yanmaz*

Department of Physics, Faculty of Arts and Sciences, Karadeniz Technical University, 61080 Trabzon, Turkey

Received 6 March 1998; received in revised form 27 May 1998

Abstract

Superconducting $YBa_2Cu_3O_x$ materials were produced by the FQMG method and their microstructures were defined by XRD analysis and optical microscopy. The optimum growth temperature and time were estimated by XRD and resistivity measurements to be 1050°C, which is in the range of the peritectic temperature of the YBCO system, and over 10 h, respectively. The effects of increasing Ag addition and applied magnetic field on the microstructure and physical properties of this system were investigated. It was found that the critical temperature ($T_{c,zero}$) of specimens slightly increased on increasing the Ag content up to 20 wt.% and the transition curves broadened on increasing the magnetic field. Additionally, the effect of oxygen annealing on the Ag-added specimens was examined and the curves of resistive transitions became sharper and $T_{c,zero}$ significantly increased.

Keywords: Ag addition; FQMG method; High-T_C superconductors; Magnetic field; Oxygen annealing; YBCO

1. Introduction

Since high-temperature superconductivity was discovered in La–Ba–Cu–O in 1986 [1] many investigations have utilized these materials for practical applications. For most applications, good superconducting and mechanical properties are desirable. In order to enhance the mechanical and electromagnetic properties, several processing methods, such as melt texture growth and chemical methods, have been used. In addition, different substitution elements or substances as a second phase in the superconductor matrix have been added for the same reasons [2].

It has been shown that the most promising method for producing large textured specimens with high critical current density (J_c) available for potential applications are the melt growth techniques [3]. The melt-powder-melt-growth (MPMG) method [4], which is a modification of the quench-melt-growth (QMG) method [5], was developed for fabricating $YBa_2Cu_3O_{7-x}$ superconducting oxides with a highly aligned structure and few weak links. It is known that the alignment of grains without weak links enhances the current carrying capacity. Another possible way of enhancing J_c is to introduce pinning sites by dispersing fine Y_2BaCuO_5 (211) inclusions in superconducting (123) grains.

$YBa_2Cu_3O_{7-x}$ pellets grown by the melt process were found to be highly dense and the microstructure is very different from that of the sintered material. The microstructure of sintered (123) consists of randomly oriented grains. The melt-textured material consists of several large domains containing parallel plates of $YBa_2Cu_3O_{7-x}$. The plates have a common *c*-axis [6].

Since the grain boundaries constitute weak links, they play an important role in the superconducting transition temperature. Anisotropic conductivity in the orthorhombic structure of the materials results in weak conductivity along the *c*-axis. About 70% of the grain boundaries in $YBa_2Cu_3O_{7-x}$ are parallel to the *c*-axis [7]. In addition, the oxygen content plays an important role in high-temperature superconductors. The critical temperature (T_c) of (123) samples depends on the oxygen deficiency. For this reason, oxygen annealing must be performed after the crystal growth process [8,9].

It has been found that silver addition enhances the critical current density (J_c), improves the transition temperature (T_c), mechanical properties and electrical stability, reduces the normal-state resistivity, enhances magnetic-flux trapping, and decreases the contact resistance. It is also know that silver improves grain growth and helps to obtain a better grain orientation. Silver addition enhances

*Corresponding author. Fax: +90-462-325-31-95; e-mail: yanmaz@osf01.ktu.edu.tr

0925-8388/98/$ – see front matter
PII: S0925-8388(98)00664-1

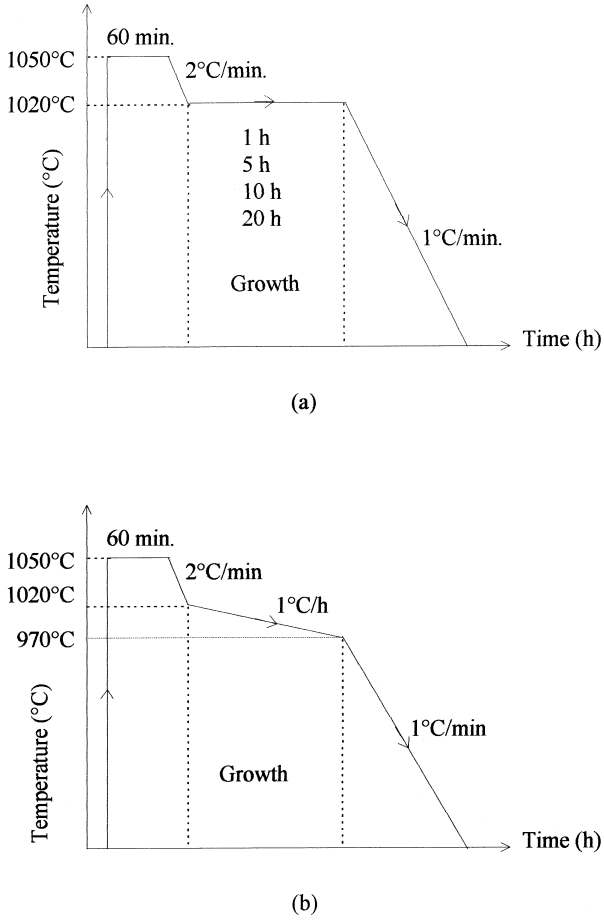

Fig. 1. Schematic representation of the heat treatment of (a) 123 and (b) Ag-added 123 prepared by the FQMG method.

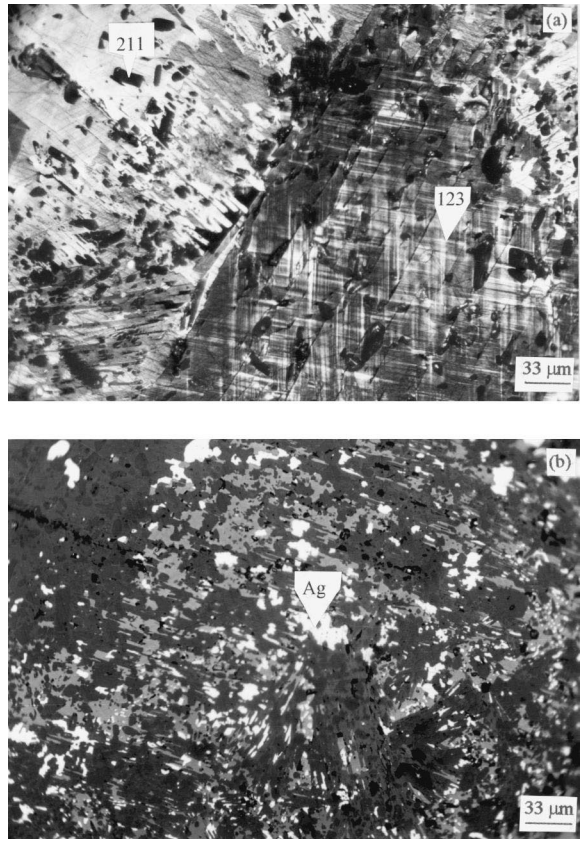

Fig. 2. Polarized light optical micrographs of (a) 123 and (b) 20 wt.% Ag-added 123.

densification, which improves the connection of superconducting grains and lowers the peritectic temperature of oxide superconductors [2,10,11].

In this paper, we report the optimum preparation conditions in terms of resistivity measurements, optical and XRD analyses for (123) specimens produced by the flame-quench-melt-growth (FQMG) method [12,13]. In addition, the temperature dependence of the resistivity in different magnetic fields, the effect of silver addition on the growth of (123) crystals and their physical properties are described.

2. Experimental procedure

Superconducting $YBa_2Cu_3O_x$ powders were prepared by mixing appropriate amounts of Y_2O_3, $BaCO_3$ and CuO using a mortar machine for 1 h to obtain an homogenous mixture. This mixture was calcined at 900°C for 8 h in air in a programmable tube furnace. After calcination, the powders were mixed for 1 h. Then, the fine powders were pressed into pellet form 13 mm in diameter and 2 mm in thickness. The pellets were melted on an Al_2O_3 substrate one by one for a short time using the flame of LPG-O_2. The molten materials were immediately poured onto a copper plate and sandwiched by another copper plate in order to sustain the formed phases during melting. These precursors were then reground for 30 min to obtain fine powders. The powders (4 g) were again pressed under a pressure of 300 MPa and then placed in a preheated furnace at various temperatures (1040, 1050, 1060, 1070 and 1100°C) for 60 min and then cooled to 30°C at a rate of 2°C min^{-1}. The samples were grown for 1, 5, 10 and 20 h in air atmosphere at this temperature. The samples were allowed to cool to room temperature at a rate of 1°C min^{-1}. Oxygen annealing was performed on all samples at 650°C for 1 h and they were then cooled to room temperature in flowing oxygen. A schematic representation of the heat treatment is shown in Fig. 1a.

In a second stage, Ag-added (123) specimens were prepared using commercial Ag powder. Ag powder was added to 4 g of quenched (123) powder in weight percentages (wt.%) of 0–30 with 5% steps. The powders were well mixed and pressed into pellets. Samples were placed in a preheated furnace at 1050°C for 60 min, then cooled to 1020°C at a rate of 2°C min^{-1} and then cooled to 970°C at a rate of 0.02°C min^{-1}. The samples were then allowed to cool to room temperature at 1°C min^{-1}. Finally,

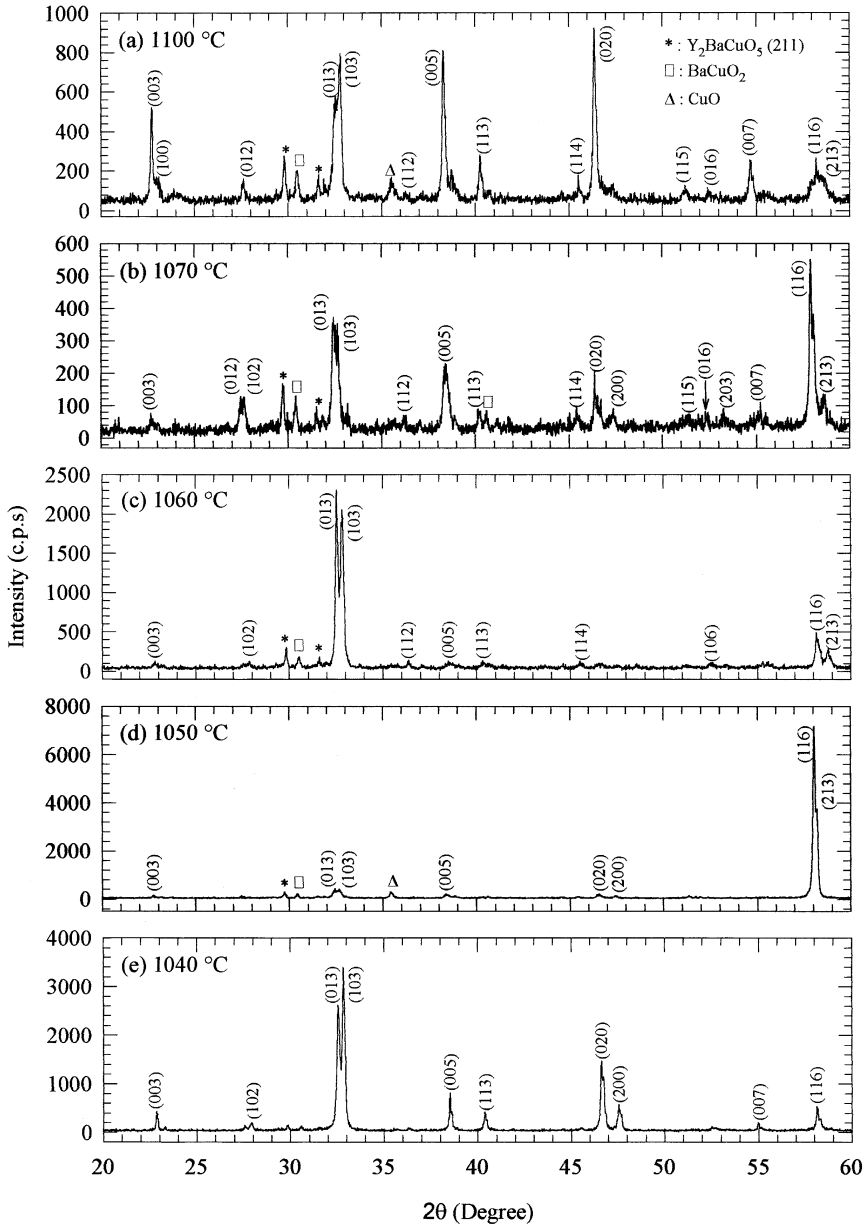

Fig. 3. Room temperature XRD patterns of 123 without Ag grown at the indicated temperatures for 10 h.

the samples were oxygen annealed at 650°C for 5 h. A schematic representation of the heat treatment is shown in Fig. 1b.

X-ray diffraction data were recorded using a Rigaku D/Max-IIIC diffractometer with Cu Kα radiation over the range $2\theta = 20–60°$. Optical micrographs of polished surfaces were taken using a polarized light microscope. The superconducting transition temperature (T_c) of samples was determined by a four-probe method. Silver paste was used as contact material. Resistivity measurements with a sensitivity of 0.01 mΩ cm were carried out using a cryostat at temperatures down to 12 K. Measurements were performed in different magnetic fields produced by an electromagnet (Walker Scientific Inc., Model HV7W; output 100 V, 50 A). The magnetic field was measured by a commercial fluxmeter.

3. Results and discussion

Fig. 2a,b show optical micrographs of polished surfaces of $YBa_2Cu_3O_{7-x}$ and $YBa_2Cu_3O_{7-x}$ with 20 wt% Ag, respectively. The micrographs indicate large-grained 123 crystals with inclusions of 211 precipitates. In Fig. 2a, the dark gray regions, which are dispersed finely in grains, represent the 211 precipitates. The precipitates can be seen in two categories: ellipsoidal and spherical. Some liquid phase (a mixture of $BaCuO_2 + CuO$) is observed at grain

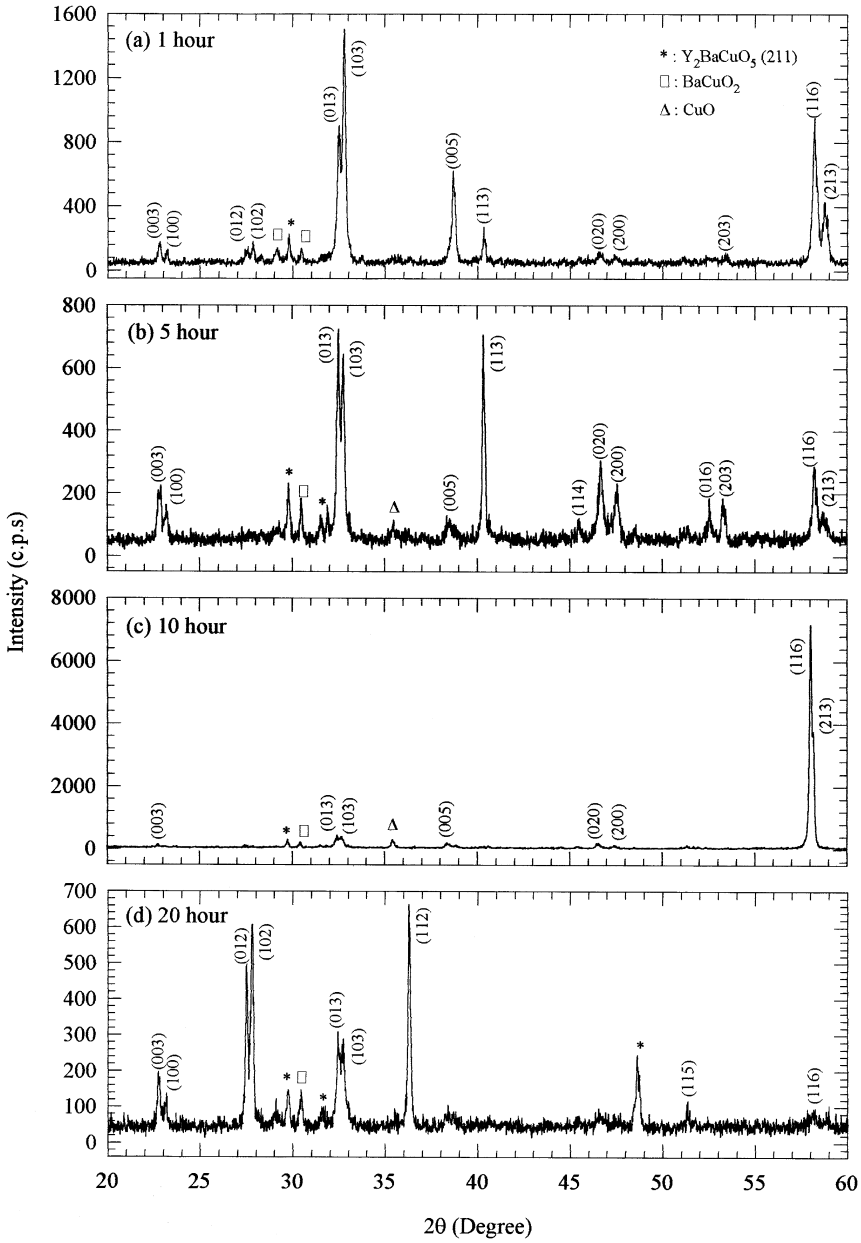

Fig. 4. Room temperature XRD patterns of 123 grown at 1050°C for the indicated times.

boundaries. A twin structure and cracks along the growth direction are also observed. It was found that the morphology of 123 is different from that of 123 with 20 wt% Ag. The bright particles seen in Fig. 2b are attributed to Ag which is dispersed homogeneously in the superconducting grains. It is thought that the Ag, which is present in grain boundaries and in grains, is not doped into the unit cell. The homogeneously distributed Ag particles can help to carry oxygen into the depth of the dense material. The grain boundaries in 123 with 20 wt% Ag were found to be cleaner without any impurity phases (211, $BaCuO_2$, CuO) than 123. The grain connectivity of Ag-added 123 is stronger. A twin structure cannot be observed in Ag-added 123. It is also observed that the amount of 211 precipitates increases with increasing silver content.

Fig. 3 shows XRD patterns of samples grown for 10 h at different temperatures. The samples were placed in a preheated furnace at temperatures of 1040, 1050, 1060, 1070 and 1100°C for 60 min and then cooled to 30°C at a rate of 2°C min^{-1}. The samples were grown at these temperatures. The main peaks belong to the 123 composition and some second phases were determined to be 211 and $BaCuO_2$ mostly at 2θ around 29° and 32°. A CuO peak was also observed at ~35.5°. It was found that the

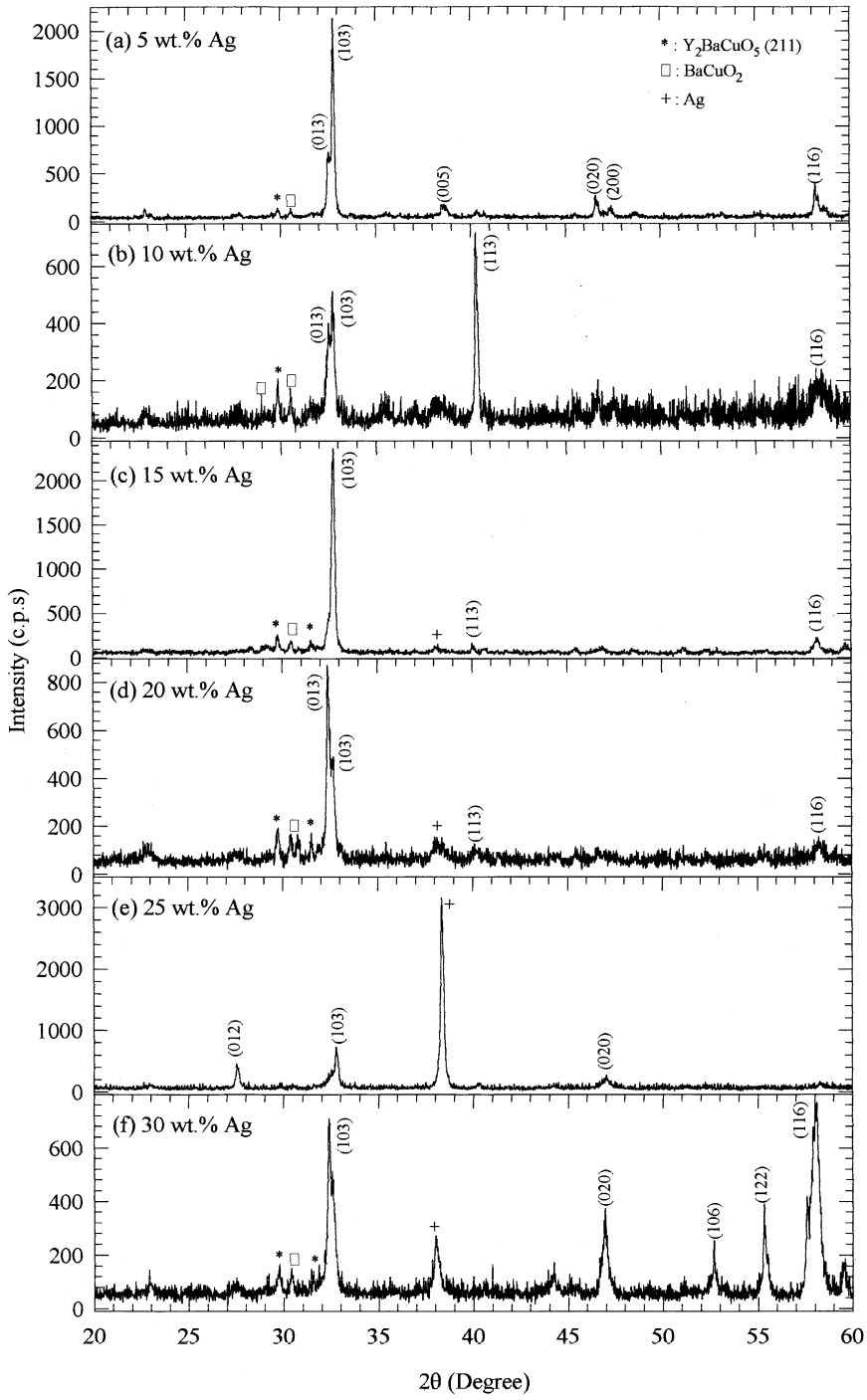

Fig. 5. Room temperature XRD patterns of 123 samples with indicated values of Ag.

amount of the second phase, which can be attributed to the start of decomposition of the 123 crystals, was increased at temperatures of 1070 and 1100°C. It can be seen from the peak profiles that the peaks of (013) and (103) at 2θ~32° were strongly affected by changing the growth temperature. The sample grown at 1050°C (Fig. 3d) shows a strong peak at 2θ~58° which indicates texturing and *c*-direction orientation of the 123 sample. It is well known that texturing and the preferred orientation of high-temperature superconductors can increase the current carrying capacity (J_c) [14].

Fig. 4 shows XRD patterns of samples grown at 1050°C for 1, 5, 10 and 20 h. The peak profiles indicate the crystal structure of the orthorhombic superconducting phase.

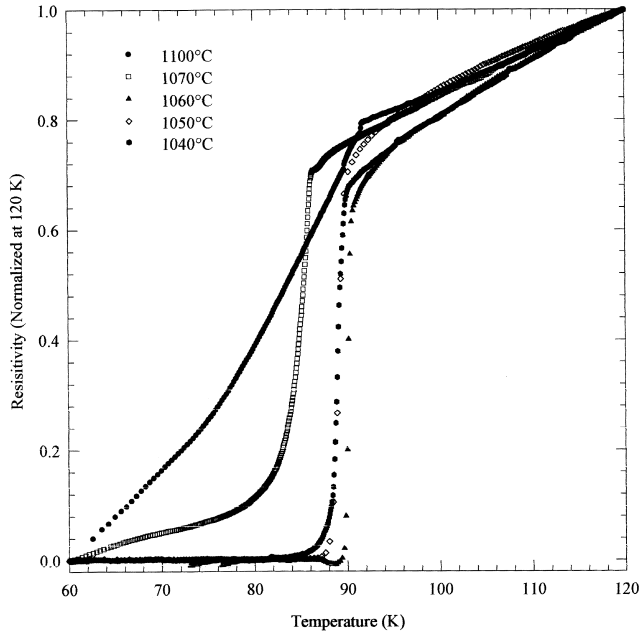

Fig. 6. Temperature dependence of the electrical resistivity for 123 samples grown as indicated for 10 h.

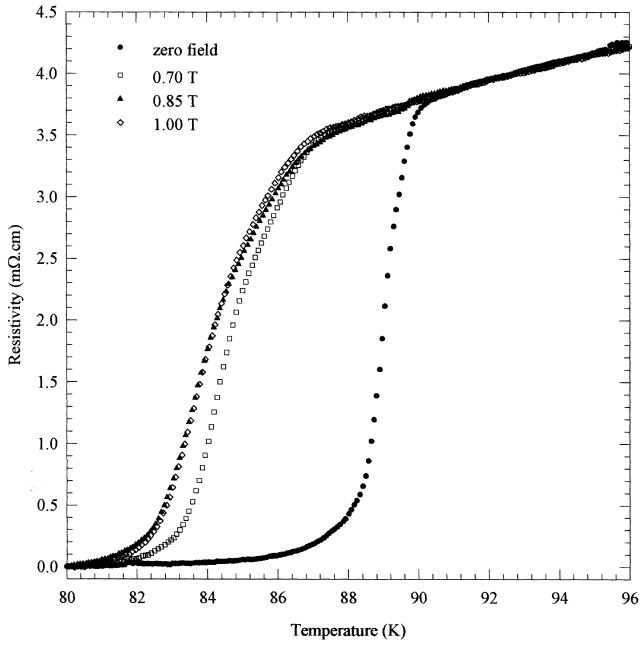

Fig. 8. Magnetic field dependence of the resistive transition of 123 grown at 1040°C for 20 h.

Some second phases of 211, $BaCuO_2$ and CuO were determined in all samples. The peak intensities as seen in Fig. 4 changed on changing the growth duration. It is thought that the growth direction of the superconducting grains changed during the growth process. The results of Figs. 3 and 4 suggest that the optimum growth temperature and time are 1050°C and >10 h, respectively.

The room temperature XRD patterns of 123 with 5–30 wt.% added Ag are shown in Fig. 5. All specimens show diffraction lines corresponding to the orthorhombic superconducting phase. The diffraction line belonging to silver is seen at $2\theta \sim 38°$ in Fig. 5c–5f. It is well known that the amount of impurity phase increases with increasing Ag content. It was reported that silver addition appreciably enhances $BaCO_3$ decomposition and the formation of the 123 superconducting phase [10]. The strongest silver peak intensity was observed for a sample with 25 wt.% silver

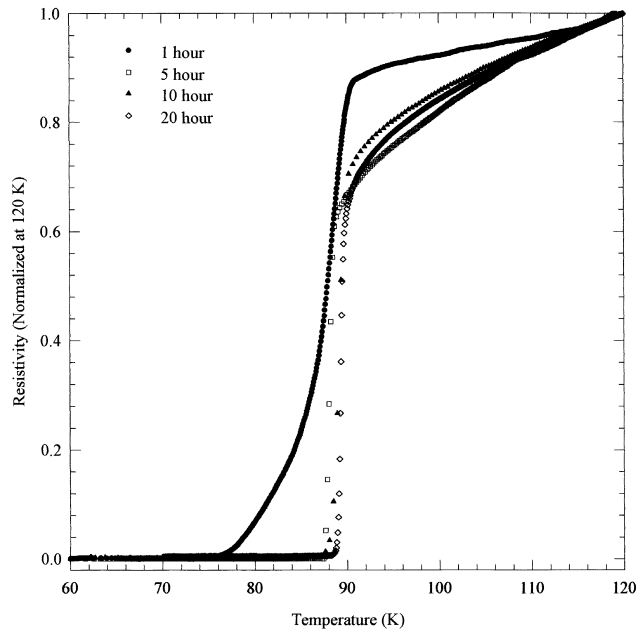

Fig. 7. Temperature dependence of the electrical resistivity for 123 samples grown at 1050°C for the indicated times.

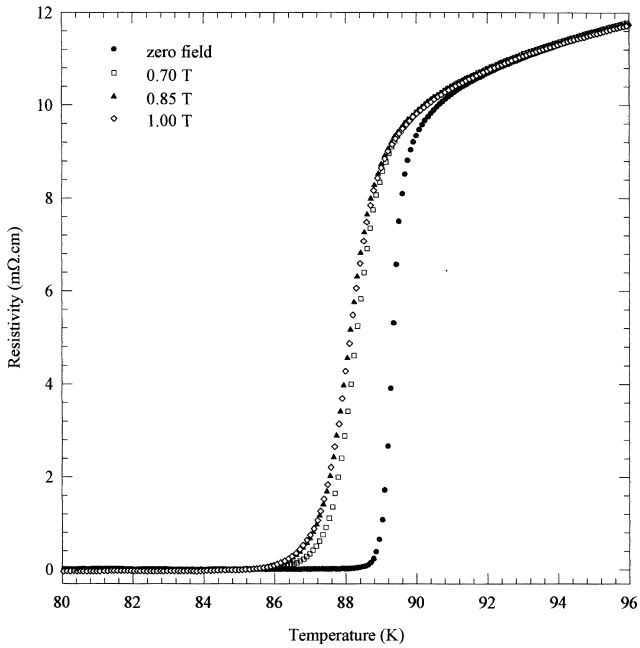

Fig. 9. Magnetic field dependence of the resistive transition of 123 grown at 1050°C for 20 h.

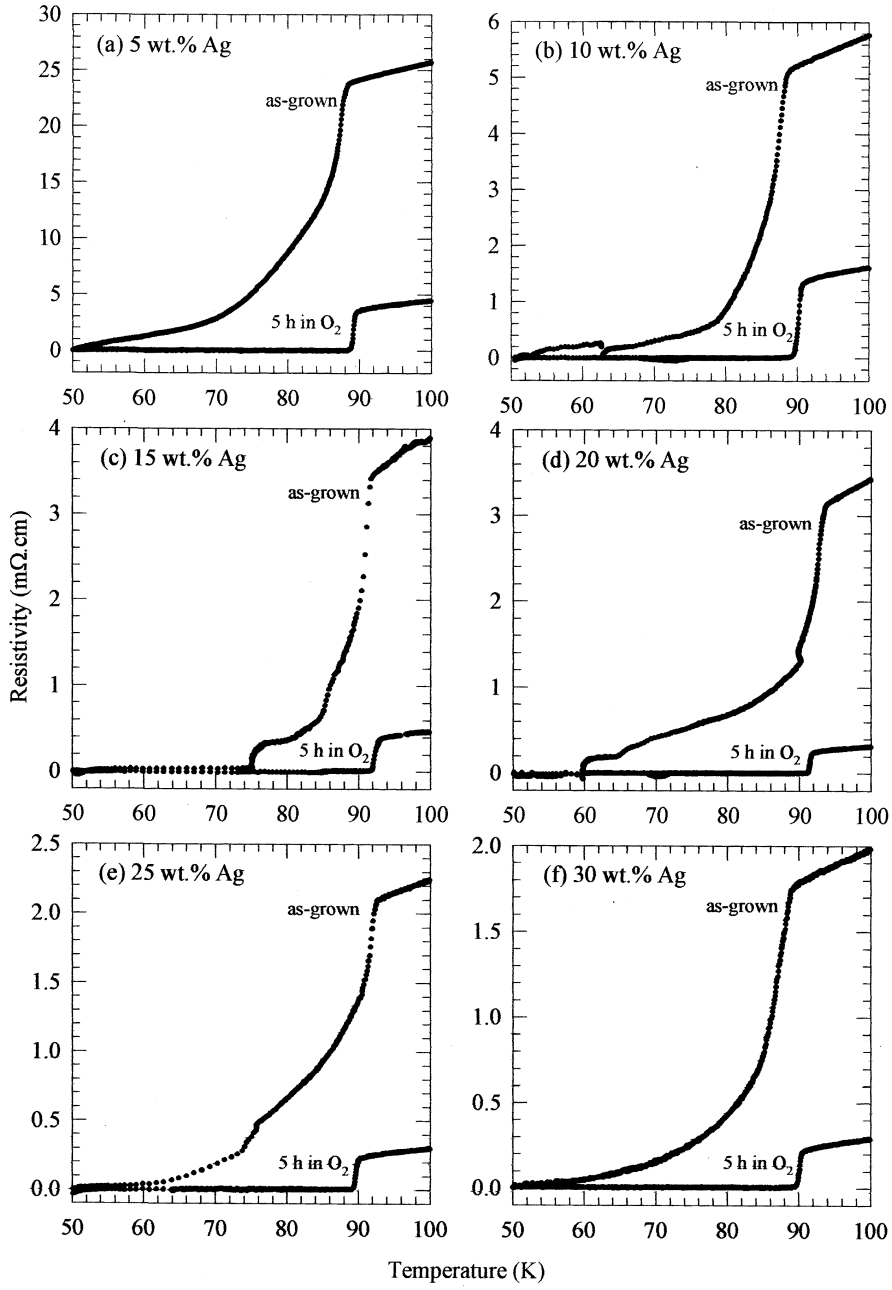

Fig. 10. Resistive transition of Ag-added 123 samples as a function of Ag content for as-grown and 5 h oxygen annealed.

(Fig. 5e). The characteristic peak intensity of (103) at ~32° is smaller than the silver peak seen at ~38°, which can be attributed to decomposition of the orthorhombic superconducting structure.

In Fig. 6, resistivity measurements are plotted to demonstrate the temperature dependence of samples grown for 10 h at 1040, 1050, 1060, 1070 and 1100°C. The best samples are those produced at 1050 and 1060°C as can be deduced from the figure. The resistivity value of the sample grown at 1060°C for 10 h was found to be 24 mΩ cm. For these samples, large grains with texturing and clean grain boundaries are observed in optical micrographs. The curves of samples grown at 1040–1060°C indicate a zero resistive critical temperature of about 90 K, which is the typical transition temperature of the 123 system. Below T_c, the curves of samples grown at 1070 and 1100°C are different at lower temperature. These curves indicate large amounts of impurity phases, such as 211, CuO and $BaCuO_2$, present in the samples and a weak connectivity between grains. The sharpness of the zero resistive transitions is proportional to the degree of interconnectivity of grains, hence the critical current density.

The duration of the growth dependence of the resistivity of the sample grown at 1050°C is shown in Fig. 7. It can be seen that the superconducting transition becomes shaper with increasing growth time. This behavior suggests that 1

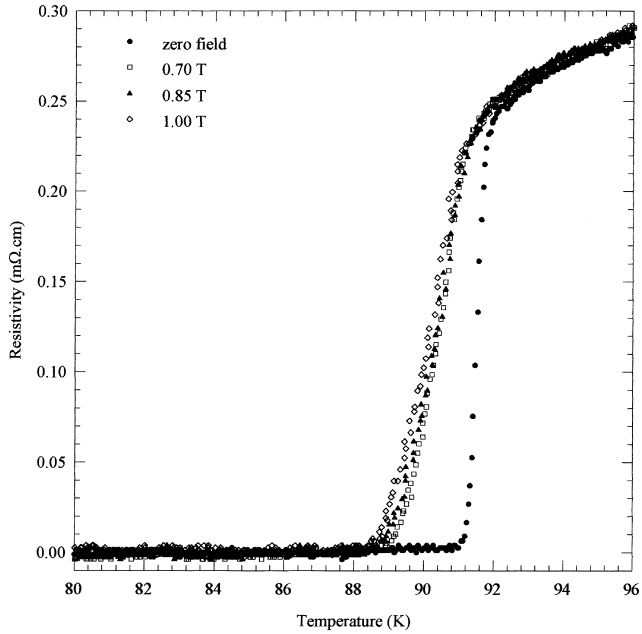

Fig. 11. Magnetic field dependence of the resistive transition of Ag-added 123 grown at 1050°C.

h of growth at 1050°C is not sufficient to complete the reaction between the 211 and liquid phases to form 123 superconducting crystals. In this work, the sharpest resistive transition at 90 K was observed in a sample grown for 20 h. This is attributed to better connectivity of grains resulting in high critical current density.

The temperature dependence of the resistivity of samples grown at 1040 and 1050°C for 20 h, measured in various magnetic fields, is shown in Figs. 8 and 9. In the field cooled (FC) procedure, the selected magnetic field was applied to the samples at room temperature. The samples were cooled to zero resistance temperature in these fields. The variation of the resistivity of the sample in these fields was recorded while the samples were heated to room temperature. The zero resistive transition temperature ($T_{c,zero}$) of the sample grown at 1040°C for 20 h (Fig. 8) was found to be 85.6 K in zero field. The value of T_c was reduced to 80.4 K when the applied field was 0.85 and 1 T. It is expected that further increases in the magnetic field will cause a further decrease in the zero resistive temperature. For the sample grown at 1050°C for 20 h (Fig. 9), the value of $T_{c,zero}$ was found to be 88.6 K in zero field and this value decreased to 86 K when the applied field was 0.85 and 1 T. Comparing these two samples in terms of durability in the magnetic field, it is clearly seen that the sample grown at 1050°C is of better quality with respect to its structural and superconducting properties.

The temperature dependence of the resistivity as a function of Ag content for as-grown and 5 h oxygen annealed 123 specimens is shown in Fig. 10. It was found that the $T_{c,zero}$ of as-grown 123 specimens with various amounts of Ag addition increased to around 90 K after oxygen annealing at 650°C. In addition, the curves of specimens became sharper and the normal-state resistivity decreased dramatically. The curves of Fig. 10c,d show the highest transition temperature of 92 K, which is the typical transition temperature of oxygen-annealed 123. The results so far suggest that oxygen annealing increases the physical properties, such as $T_{c,zero}$ and J_c, of YBCO superconductors. It is well known that YBCO superconductors are oxygen deficient in their crystal structure. It has been reported that the oxygen deficiency decreases the pinning in polycrystalline YBCO material [15] and reduces the condensation energy of this material resulting in a decrease of the critical current density (J_c) and pinning of vortices [16]. In addition, the decrease in the superconducting transition temperature (T_c) is due to a disordering of the oxygen chains, which plays a major role in the mechanism of high-temperature superconductivity. It is also known that melt-textured material is rather dense. It can also be speculated that oxygen can be transported deep into the sample by silver. Hence, the oxygen annealing treatment must be performed in order to incorporate sufficient oxygen to achieve a high critical temperature (T_c).

Fig. 11 shows the resistive transition of a 20 wt.% Ag-added 123 specimen for different values of the magnetic field in the FC procedure. It is seen that the $T_{c,zero}$ of 91 K decreases significantly with increasing magnetic field, for example 88.5 K at 1 T. It can clearly be seen that the $T_{c,zero}$ of 88.6 K in zero field in the FC procedure for the specimen grown at 1050°C for 20 h with no silver (Fig. 8) increased to 91 K (Fig. 11), which is an indication of an increase in $T_{c,zero}$ on adding Ag to the YBCO superconducting material.

Acknowledgements

This work was supported by the Research Fund of Karadeniz Technical University, Trabzon, Turkey.

References

[1] J.G. Betnorz, K.A. Müller, Z. Phys. B, Condensed Matter 64 (1989) 189.
[2] F.C. Fonseca, R. Muccillo, Physica C 267 (1996) 87.
[3] I. Monot, J. Wang, M.P. Delamare, J. Provost, G. Desgardin, Physica C 267 (1996) 173.
[4] M. Murakami, T. Oyama, H. Fujimoto, S. Gotoh, K. Yamaguchi, Y. Shiohara, N. Koshizuaka, S. Tanaka, IEEE Trans. Magn. 27(2) (1991) 1479.
[5] M. Murakami, Mod. Phys. Lett. B 4(3) (1990) 163.
[6] E. Sudhakar Reddy, T. Rajasekharan, Physica C 279 (1997) 56.
[7] A. Singh, P. Kuppusami, E. Mohandas, S. Raju, V.S. Raghunathan, Physica C 261 (1996) 273.
[8] N. Chikumoto, S. Ozawa, S.I. Yoo, N. Hayashi, M. Murakami, Physica C 278 (1997) 187.
[9] A. Wisniewski, C. Czurda, H.W. Weber, M. Baran, M. Reissner, W. Steiner, P.X. Zhang, L. Zhou, Physica C 266 (1996) 309.

[10] A. Sen, H.S. Maiti, Physica C 229 (1994) 188.
[11] Ch. Zhang, A. Kulpa, A.C.D. Chaklader, Physica C 252 (1995) 67.
[12] A. Gencer, A. Ateş, E. Aksu, S. Nezir, S. Çelebi, E. Yanmaz, Physica C 279 (1997) 165.
[13] A. Ateş, E. Yanmaz, S. Çelebi, J. Alloys Comp. 268 (1998) 215.
[14] M. Murakami, Supercond. Sci. Technol. 5 (1992) 185.
[15] H. Theuss, H. Kronmüller, Physica C 177 (1991) 253.
[16] J.G. Ossandon, J.R. Thompson, D.K. Christen, B.C. Sales, H.R. Kerchner, J.O. Thomson, Y.R. Sun, K.W. Lay, J.E. Tkaczyk, Phys. Rev. B 45 (1992) 12534.